Effects of mild thermal pre-treatment combined with H_2O_2 addition on waste activated sludge digestibility

Gonzalez, Adrian; van Lier, Jules B.; de Kreuk, Merle K.

DOI
10.1016/j.wasman.2022.01.017

Publication date
2022

Document Version
Final published version

Published in
Waste Management

Waste Management 141 (2022) 163–172

Contents lists available at ScienceDirect

Waste Management

journal homepage: www.elsevier.com/locate/wasman

Effects of mild thermal pre-treatment combined with H_2O_2 addition on waste activated sludge digestibility

Adrian Gonzalez *, Jules B. van Lier, Merle K. de Kreuk

Faculty of Civil Engineering and Geosciences, Department of Water Management, Sanitary Engineering Section, Delft University of Technology, Stevinweg 1, 2628 CN Delft, the Netherlands

ARTICLE INFO

Keywords:
Apparent viscosity
Catalase activity
Cationic polymer
Hydroxyl radicals
Low-temperature pre-treatment
Non-ideal mixing

ABSTRACT

The pre-treatment of waste activated sludge (WAS) has become more common since it often results in improved bioconversion to methane, in both rate and extent. However, thorough insights on the possible effects and mechanisms of mild pre-treatment techniques, such as temperatures <100 °C combined with the addition of H_2O_2, are still limited. This study reports the effects of the addition of 5–30 mgH_2O_2/g TS and its interaction with thermal pre-treatment at 70 °C on methane production, using WAS as the substrate. It was found that the addition of H_2O_2 increased the methane production rate, coinciding with a decrease in apparent viscosity of WAS, which probably improved mass transfer under non-ideal mixing conditions. While H_2O_2 solubilized proteins and carbohydrates and mineralized a small fraction of the humic substances in WAS, these biochemical transformations did not suffice to explain the observed extent and rate of methane production. A decreased particle size, the presence of Fenton's reagent, and the presence of cationic polymers in the WAS were discarded as the reasons for the observed decrease in apparent viscosity. It was concluded that the pre-treatment conditions applied in the present study might be a strategy to enhance mixing conditions in full-scale anaerobic digesters.

1. Introduction

Waste activated sludge (WAS) is the main by-product of conventional activated sludge (CAS) wastewater treatment plants (WWTP). Around 14–17 kg as dry solids per person per year are produced in the European Union, Japan and Australia and up to 55 kg TS per person per year in the United States, where kitchen grinders are commonly used (Wu et al., 2020). Due to its putrescible nature, WAS requires a proper disposal, which is commonly achieved via anaerobic digestion (AD) and subsequent landfilling or incineration. The treatment of WAS before AD (WAS pre-treatment) commonly results in improved biogas production, dewatering and hygienization (A. Gonzalez et al., 2018; Neumann et al., 2016). In particular, thermal pre-treatment techniques have been popularized and are commonly categorized into high- and low-temperature using 100 °C as division. In this regard, low-temperature thermal pre-treatment has a lower energy requirement and avoids the use of pressured vessels, steam and sophisticated control systems (Pilli et al., 2014). Various studies have combined low-temperature thermal pre-treatment with chemical reagents, such as hydrogen peroxide (H_2O_2) to potentiate the benefits of pre-treatment. For instance, pre-treatment using microwaves combined with H_2O_2 has resulted in synergetic increases in methane production rate and extent, sludge stabilization and a decrease in apparent viscosity of sludge and digestate (Ambrose et al., 2020; Liu et al., 2016; Wang et al., 2009). The observed effects of microwave-H_2O_2 pre-treatment have been attributed to oxidizing by-products or side-reactions, such as Fenton's reagent and superoxide radicals (Ambrose et al., 2020; Xiao et al., 2012; Yu et al., 2016). Nonetheless, such claims have not been thoroughly researched, probably because of the difficulty of measuring oxidizing species such as hydroxyl radicals. In addition, it is unclear how each pre-treatment individually contributes to the reported improvements in solubilization, methane production and to the decreased WAS viscosity.

In our present research, convectional thermal pre-treatment at 70 °C was used instead of microwaves, since the application of temperature via microwave irradiation or heating via convection has yielded similar results (Eskicioglu et al., 2007; A. Gonzalez et al., 2018). In view of any possible full-scale application, convectional heat is considered more cost-effective, as it avoids the capital cost and electricity consumption of microwave equipment. The objective of our present work is to clarify the effects of convectional thermal pretreatment at 70 °C combined with H_2O_2 addition on WAS, as well as to provide insights about the previously-reported increases in methane production.

* Corresponding author.
E-mail address: J.A.GonzalezOrtega@tudelft.nl (A. Gonzalez).

https://doi.org/10.1016/j.wasman.2022.01.017
Received 28 September 2021; Received in revised form 23 December 2021; Accepted 14 January 2022
Available online 3 February 2022

2. Methods

2.1. Sludge origin and characteristics

WAS was obtained from the wastewater treatment plant Kralingseveer (KV) (Rotterdam, The Netherlands) in September (autumn). The sludge was collected after the centrifugation step and therefore included the conditioning agent (cationic polymer) VTA LC 186 (VTA Austria GmbH, Austria). Physicochemical characteristics of WAS were as follows: TS = 79.7 g/L; VS = 56.8 g/L; COD = 86.1 g/L. The same WAS batch was pre-treated (see Section 2.2) in multiple events to ensure sufficient sludge was available to perform all the analytical assays. In addition, samples from two other wastewater treatment plants were taken to perform rheometric assays: Nieuwgraaf (NG) (Arnhem, The Netherlands), with TS = 61.2 g/L and VS = 48.1 g/L and Harnaschpolder (HP) (Den Hoorn, The Netherlands), with TS = 53.2 g/L and VS = 41.9 g/L. Digestate was obtained from Harnaschpolder treatment plant, with TS = 35.3 g/L and VS = 25.4 g/L. The anaerobic digesters in Harnaschpolder were operated with a retention time of ~21 days at 37 °C.

2.2. WAS pre-treatment

Thermal pre-treatment of WAS was performed as shown in Gonzalez et al., (2021). H_2O_2 at a concentration of 30% w/w (Merck, U.S.A.) was dosed according to the designated concentrations. In the pre-treatments without H_2O_2, demineralized water was added to balance the liquid volume. In addition, the added water also compensates the production of water after H_2O_2 addition (Eq. (1)). The amount of added water always was <2 mL or <0.5% of the total WAS mass.

$$2H_2O_2 \rightarrow 2H_2O + O_2 \quad (1)$$

Since the dosage strategy or sequence of H_2O_2 application has been observed to markedly influence the outcomes of pre-treatment (Ambrose et al., 2020; Gan and Li, 2013; Pignatello et al., 2006), the addition of either H_2O_2 or water proceeded 10 min after WAS reached a temperature of 70 °C; then the temperature was maintained for 30 min. The chosen strategy agrees with Wang et al. (2009) and is based on the rationale that pre-incubation at 70 °C would lead to denaturation of catalase before H_2O_2 is added. In addition, the time lapse of 20 min at 70 °C after H_2O_2 addition would promote fast decomposition of H_2O_2 (Wu and Qian, 2018), preventing peroxide from entering the anaerobic digesters. Oxidation-reduction potential (ORP) was chosen as surrogate for H_2O_2 detection, since photometric detection of H_2O_2 from the WAS matrix probed to yield into stoichiometrically impossible concentrations, probably due to interferences. Temperature, pH and ORP were carefully measured during each pre-treatment to ensure similar pre-treatment conditions for each pre-treatment event, as detailed next.

2.3. Analytical

2.3.1. COD, pH, solids, VFA, ORP and pH

Total solids (TS); volatile solids (VS); chemical oxygen demand (COD); and volatile fatty acids (VFA) were measured as described previously (Gonzalez et al., 2020). pH was measured with a SenTix 940 IDS probe (WTW, Germany) and oxidation–reduction potential (ORP) with a SenTix ORP-T 900 (WTW, Germany). The pH probe was calibrated daily and the ORP probe was checked for accuracy with a standard solution before each use. Data was captured with a multimeter model 3620 IDS (WTW, Germany). Finally, temperature was measured with two digital thermometers model G1710 (Greisinger, Germany).

2.3.2. Rheometry

Shear stress and shear rate were measured using a rotational rheometer model MCR 302 (Anton Paar GmbH, Graz, Austria) with a smooth measuring cylinder model B-CC27 with a diameter of 26.66 mm and a measuring cup model C-CC27 with a diameter of 30 mm. The volume of the sample was ~17 mL and the assays were performed at 35 ± 0.2 °C and lasted ~3 min. A shear rate from 0.01 to 1000 s^{-1} with a logarithm curve was applied, without a pre-shearing stage. The obtained rheograms were fitted to the Herschel-Bulkley model, which has been observed to be a suitable model for non-Newtonian fluids such as concentrated WAS (Liu et al., 2016; Wei et al., 2018) (Eq. (2)):

$$\tau = \tau_y + k\gamma^n \quad (2)$$

Where:

τ = shear stress, Pa
τ_y = yield stress, Pa
k = consistency index, Pa•s
γ = shear rate, s^{-1}
n = flow behavior index, unitless

Storage and loss moduli (G′ and G″, respectively) describe the elastic and viscous properties of viscoelastic materials. G′ relates to the solid-like behavior and G″ to the liquid-like behavior of a sample (Anton-Paar, 2021) (Eqs. (3) and (4)). The strain at which G″ = G′, is the deformation required for the sample to start behaving from a solid-like to a liquid-like behavior.

$$G' = \frac{\sigma_0}{\varepsilon_0} cos\delta \quad (3)$$

$$G'' = \frac{\sigma_0}{\varepsilon_0} sin\delta \quad (4)$$

Where:

G' = storage modulus, Pa
G'' = loss modulus, Pa
σ_0 = initial stress, Pa
ε_0 = initial strain, m/m
δ = phase-shift angle

Both G′ and G″ were measured using a stainless-steel plate model I-PP80/SS with a diameter of 80 mm and a cone plate model CP50 with a diameter of 50 mm, an angle of 1.001° and a truncation of 102 µm. Both implements were manufactured by Anton Paar (Anton Paar GmbH, Graz, Austria). Around 3 mL of WAS were used and the temperature was controlled at 35 ± 0.2 °C. The strain was logarithmically applied from 0.01% to 100%. The duration of each assay was ~5 min.

2.3.3. Particle size distribution (PSD)

A laser diffraction instrument model Microtrac MRB's Bluewave (Microtrac Retsch GmbH, Germany) was used to measure PSD. The WAS samples were diluted 1:5 with a solution of 0.05% NaCl (w/v) and analyzed.

2.3.4. Catalase activity test

Catalase activity assay was based on the method of Iwase et al. (2013). Briefly, a sample of unknown concentration of catalase, surfactant and H_2O_2 are combined in a test tube. The oxygen generated by the enzymatic decomposition of H_2O_2 is trapped by the surfactant, producing foam. The height of the foam column is proportional to the concentration of catalase and is related to a calibration curve. Catalase from bovine liver (CAS 9001-05-2 with 2000–5000 units/mg protein, and 65% protein) from Sigma (Sigma-Aldrich, U.S.A.) was used as standard. Solutions of catalase with concentrations of 0, 25, 50 and 100 enzymatic units (U) were prepared for the calibration curve. Triton X-100 from Sigma was used as surfactant and H_2O_2 at a concentration of 30% w/w was obtained from Merck (U.S.A.). WAS was diluted 1:5 and 0.1 mL were added to a test tube model 114,724 from Merck. Then, 0.1

mL of 1% Triton X-100 was added together with 0.1 mL of H_2O_2. All the dilutions were performed with demineralized water. The test tube was gently stirred by hand and allowed to rest for 5 min at 20 °C. Finally, the height of foam was measured with a ruler and compared with the standard curve. The analysis was performed in triplicates.

2.3.5. Measurement of hydroxyl radicals. Quantification of HO radicals (HO•) proceeded as follows

Disodium terephthalate (Na_2TA) (Alfa Aesar, U.S.A) was used as a molecular probe (Charbouillot et al., 2011; D. Gonzalez et al., 2018) at a Na_2TA:Fe molar ratio of 2. Depending on the experiment, either H_2O_2 or water was added to the WAS and the sludge was held for 30 min at 70 °C. A sample of 25 g of pre-treated sludge was diluted 1:2 with demineralized water and centrifuged at 15,000*g* (gravitational acceleration units) for 10 min using a centrifuge model Sorvall ST 16 (Thermo Fisher Scientific, U.S.A.). The supernatant was filtered through a polytetrafluoroethylene (PTFE) filter (Macherey-Nagel GmbH & Co, Düren, Germany) with a nominal pore-size of 0.45 μm. The filtered sample was then pipetted into a well of a 96-well Bio-One Cell star microplate (Greiner Bio-One GmbH, Austria) and analyzed with a spectrophotofluorometer model Polar Star Optima, (BMG Lab Tech, U.S.A.). The reaction between Na_2TA and HO• results in 2-hydroxyterephtalate (2hTA), which is detected at (λ_{exc} = 320 nm and λ_{em} = 420 nm) (Fang et al., 1996). A calibration curve was prepared with 2hTA obtained from Sigma at concentrations of 0.0, 2.5, 5.0 and 7.5 μM. The yield of the reaction between HO• and 2hTA was assumed to be 35% for samples containing H_2O_2 (Fang et al., 1996) and 87% for samples without H_2O_2 (Charbouillot et al., 2011). To validate the viability of the probe, WAS was exposed to 70 °C with 15 mg H_2O_2/g TS and sonicated with a digital sonicator model 250 (Branson Ultrasonics Corp., U.S.A 250) with a frequency of 20 kHz and at a specific energy of 3.06 kW/g TS. Sonication is an established method for the production of HO• (Le et al., 2015; Pilli et al., 2011). The duration of the sonication was 30 min and the temperature increase was <1 °C. The sonicated sample was compared to a non-sonicated control. Compared to control, the sonicated sample had a higher concentration of Na_2TA (Fig. S1), demonstrating the sensitivity and suitability of Na_2TA for the quantification of HO•.

2.3.6. Methane production rate (k_{CH4}) and specific methane production (SMP)

k_{CH4} and SMP were determined as described previously (Gonzalez et al., 2020). SMP values are reported as volume of methane per gram of added VS of the un-treated WAS; that is, without considering any possible mineralization of sludge as a result of pre-treatment. Regarding the first order kinetic model, a two-substrate model was used, using as division the best apparent curve fitting. Anaerobic digestate was mixed with a substrate to inoculum ratio of 1:2 (as VS). Two SMP tests were performed: the objective of the first set was to compare the SMP of a) non-treated WAS; b) WAS pre-treated at 70 °C; and c) WAS at 70 °C with 15 mg H_2O_2/g TS. Digestate (see Section 2.1) was degassed for 7 days at 35 °C. Bottles with a working volume of 400 mL were agitated with an orbital incubator shaker model Innova 40 (Eppendorf, Germany) at a rotational speed of 120 rpm at 35 °C. The produced biogas was scrubbed with 80 mL of 3 M NaOH solution and the exit gas was measured in a gas volume measuring device (BPC, Sweden). Crystalline cellulose (Sigma-Aldrich, U.S.A.) was used as a control substrate and tap water was added to the bottles containing the control and blank samples until all the bottles had a similar head space. The objective of the second SMP test was to compare the effects of different mixing regimes and WAS rheology on the production of methane. The test consisted of 30 bottles (each with a working volume of 400 mL): half of them were mixed with an orbital incubator shaker model Innova 44 (Eppendorf, Germany) with a rotational speed of 120 rpm. The other bottles were stirred with the Multifunction Brushless DC motor included in the AMPTS-II (BPC, Sweden). For each mixing mode, a cellulose control was prepared as described above. The rotational speed of the AMPTS-II motors was set to ~160 rpm for each motor and was monitored with a tachometer model DT-30LK (Voltcraft, Germany). The stirring cycle was: 5 min on; 30 s off, with alternative bidirectional mixing. For each mixing regime, the temperature was monitored at 35.0 ± 0.2 °C. For the second test, digestate was stored for 4 days at 4 °C.

2.3.7. Extracellular polymeric substances (EPS) extraction

EPS composition; and *Inductively Coupled Plasma Optical Emission Spectrometry (ICP-OES)*, were performed as described in Gonzalez et al., (2021) in order to determine the Fe concentration in WAS.

2.3.8. Viscosity of solutions of model molecules

Solutions of food-grade hydrolyzed collagen (Plent, Schagen, The Netherlands); analytical-grade humic acid sodium salt (Sigma-Aldrich, U.S.A); and analytical-grade crystalline cellulose (Carl Roth GmbH & Co KG, Germany) were prepared as model molecules of protein, humic substance and carbohydrates, respectively. Demineralized water was used to prepare the solutions, which were as concentrated as possible but still able of being mechanically mixed with magnetic stirrers. The resulting TS concentrations and VS fractions were: 411 mg collagen/g at 96% VS; 305 mg humic acid/g at 27% VS; and 269 mg cellulose/g at 100% VS. 80 mL of each solution, were exposed to the same conditions as the pre-treatment settings shown in Section 2.2 and the resulting broths were subjected to rheometric assays as shown in Section 2.3.2.

3. Results and discussion

3.1. Physicochemical parameters

During pre-treatment, the breakdown of H_2O_2 by catalase (the enzyme that mediates the decomposition of H_2O_2 into water and oxygen) (Wang et al., 2009) will result in misused reagent; thus, catalase must be inactivated via thermal denaturation to ensure H_2O_2 is available for other reactions. Previous research showed that catalase is denatured at temperatures ranging from 60 to 80 °C, depending on the time of exposure (Eyster, 1950; Liu et al., 2015; Velayati et al., 2019). In the present study, the effects of temperature on the activity of catalase were clearly observed (Fig. S2a and b); catalase activity was no longer present after only 2 min of exposure to a temperature of 70 °C (Fig. S2b).

The decomposition of H_2O_2 and its possible oxidizing derivatives were monitored via oxidation–reduction potential (ORP) measurements. Dewatered WAS showed a negative ORP (reducing conditions) due to the high oxygen-consuming activity of the activated sludge. Fig. 1a shows that the exposure of WAS to 70 °C only caused a marginal increase in ORP that likely can be ascribed to intensive mixing during pre-treatment, which induced aeration of the sample. As expected, the application of H_2O_2 sharply increased the ORP until oxidizing conditions (Fig. 1b) but the ORP decreased smoothly to a reducing environment after 9–12 min of dosing, suggesting the progressive decomposition of H_2O_2 and its possible oxidizing by-products, thus preventing their entrance to anaerobic digesters. Fig. 1c shows an increase in temperature of almost 2 °C, indicating the exothermic nature of the reaction between H_2O_2 and the WAS components. The pH decreased almost 1 unit during pre-treatment with or without H_2O_2 (Fig. 1d), which coincided with the formation of VFAs during thermal pre-treatment. Nonetheless, the observed decline in pH (<1 unit) seems insufficient to attribute any potential effect of H_2O_2 to a pH-related mechanism, although a small but sharp drop coincided with H_2O_2 addition.

After pre-treatment, the concentration of solids and COD of the sludge samples was analyzed. Fig. S3 shows that H_2O_2 provoked a slight decrease in TS, VS and COD, suggesting mineralization of organic matter (Eskicioglu et al., 2008; Xiao et al., 2012). Based on the COD mass balance and the redox half-reactions of H_2O_2, it was calculated that the number of electrons donated by the sludge was>8 times higher than the potentially scavenged electrons by the dosed H_2O_2 (Annex A in Supplementary Information), suggesting that some mineralization indeed

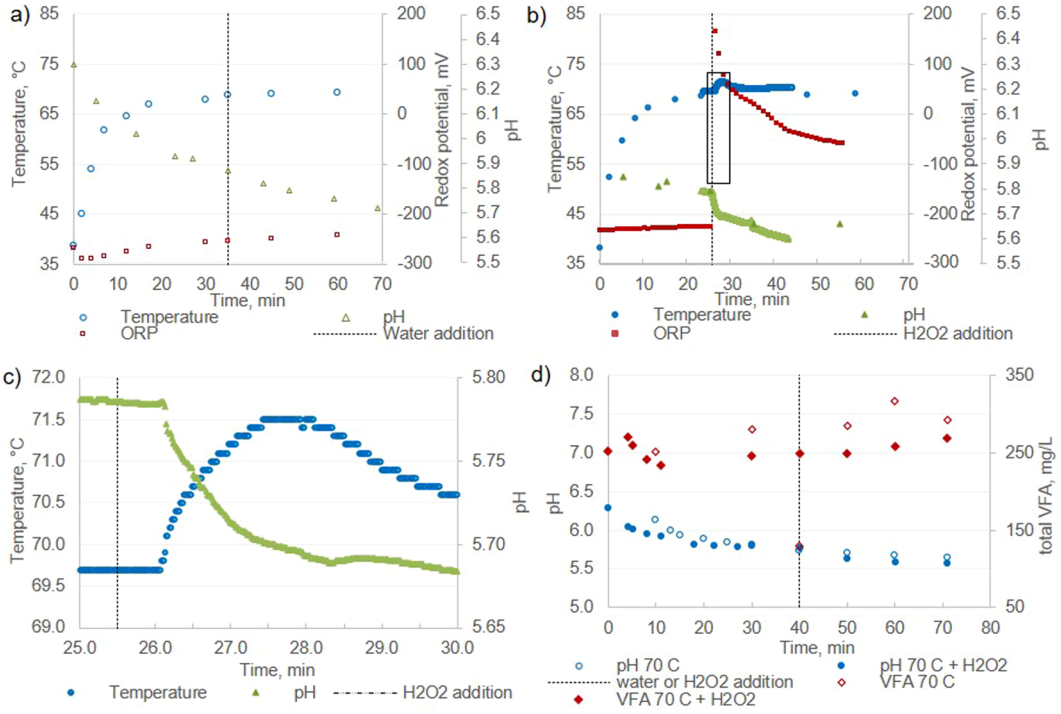

Fig. 1. Temperature, pH and ORP of WAS during pre-treatment at a) 70 °C; b) 70 °C with 15 mg H_2O_2/g TS, (squared area is shown in c); c) zoom of squared areas in b; and d) pH and VFA of sludge pre-treated at 70 °C with and without H_2O_2.

occurred during pre-treatment. The occurrence of mineralization reactions may be explained by an increased effectiveness of H_2O_2, due to the absence of catalase and the increased H_2O_2 reaction rate at the applied temperature.

3.2. EPS

The exposure of WAS to 70 °C resulted in a marked increase in concentration of extractable proteins, humic substances and carbohydrates and a shift of these compounds from the tightly bound fraction to the loosely and soluble fraction (Fig. 2a–c). These trends coincide with previous reports under similar pre-treatment conditions (Liang et al., 2020; Zhen et al., 2019). However, while the addition of 15 mg H_2O_2/g TS triggered a further increase in the concentration of extractable proteins and carbohydrates (Fig. 2a and c), there was a slight decrease in the concentration of humic substances when the sludge was exposed to H_2O_2 (Fig. 2b). Humic acids are less soluble under acidic conditions. However, both pre-treatment conditions resulted in similar pH drops, although the H_2O_2-treated samples had a more abrupt decline immediately after the addition of peroxide (Fig. 1a and b). The decrease in extractable humic substances was also observed when the experiment was repeated using a different sludge sample (Fig. S4). Based on the observed results, it was postulated that H_2O_2 degraded a fraction of the humic substances in WAS, which resulted in the observed decrease in VS and COD (Fig. S3). In previous studies, the degradation of humic matter was observed after the application of H_2O_2 during microwave pre-treatment of WAS (Eskicioglu et al., 2008) and lignite (Doskočil et al., 2014).

3.3. Rheology

As reported for similar temperatures (Hammadi et al., 2012; Wei et al., 2021), the exposure of WAS to 70 °C resulted in an overall decrease in shear stress at shear rates 0.01–1000 s^{-1} (Fig. 3a and Fig. S5). However, the addition of 5–30 mgH_2O_2/g TS provoked a further decrease in shear stress, and thus, in the apparent viscosity of WAS, particularly in the shear rate range that is considered typical for the flow velocity gradients in full scale digesters (0.14–1.0 s^{-1})(Fig. 3b) (Dapelo and Bridgeman, 2018; Wei, 2021). A decrease in apparent viscosity was also reported by Liu et al. (2016), using microwave heating at 100 °C, with a 10-fold higher H_2O_2-dose than in the present study.

Previous studies have shown that the rheological properties of the fermentation liquor impact the mass transfer and short-circuiting during mixing in both lab- and full-scale digesters (Liu et al., 2018; Samstag et al., 2016; Wei et al., 2019). In addition, sludge viscosity impacts the economics of sludge management since it influences mass-transfer rates (Liu et al., 2018; Ratkovich et al., 2012): the lower the apparent viscosity of the fermentation liquor, the better the mixing performance, the higher the biogas production rate, and the lower the occurrence of dead-zones under non-ideal mixing conditions (Liu et al., 2018; Miryahyaei et al., 2019; Wei et al., 2019).

Moreover, the consistency index *k* (which is a proxy of viscosity)(Eq. (2)) and the loss modulus G'' (Eq. (4)) have been demonstrated as indicators for the level of biogas production in lab-scale experiments (Miryahyaei et al., 2019). Thus, it was hypothesized that the decrease in *k*, G'', and WAS yield stress (τ_y), might result in increased biogas production as studied in Section 3.4. The parameters of the Herschel-Buckley model (Eq. (2)) were calculated via curve fitting of the rheograms in Fig. 3. The fitted curves and tabulated values are shown in Fig. S6 and Table S1.

Fig. 4a shows a clear decrease in consistency index with a dose of 5 mg H_2O_2/g TS, and a further modest decrease was observed proportional to the concentration of H_2O_2. Apparently, WAS viscosity lowered in proportion to the dose of H_2O_2. Similarly, also the yield stress for WAS dosed with 5 mg H_2O_2/g TS decreased; however, there was no additional decrease for higher H_2O_2 doses. The flow behavior index (n) had a constant increase in proportion to the H_2O_2 concentration (Fig. 4b), suggesting that the pre-treated WAS became a more Newtonian fluid with every increase in H_2O_2 concentration. Overall, our results indicate that the WAS pre-treated with H_2O_2 increased its fluidity, which is in line with the findings of Liu et al. (2016), which were obtained with a 10-fold higher H_2O_2 dose.

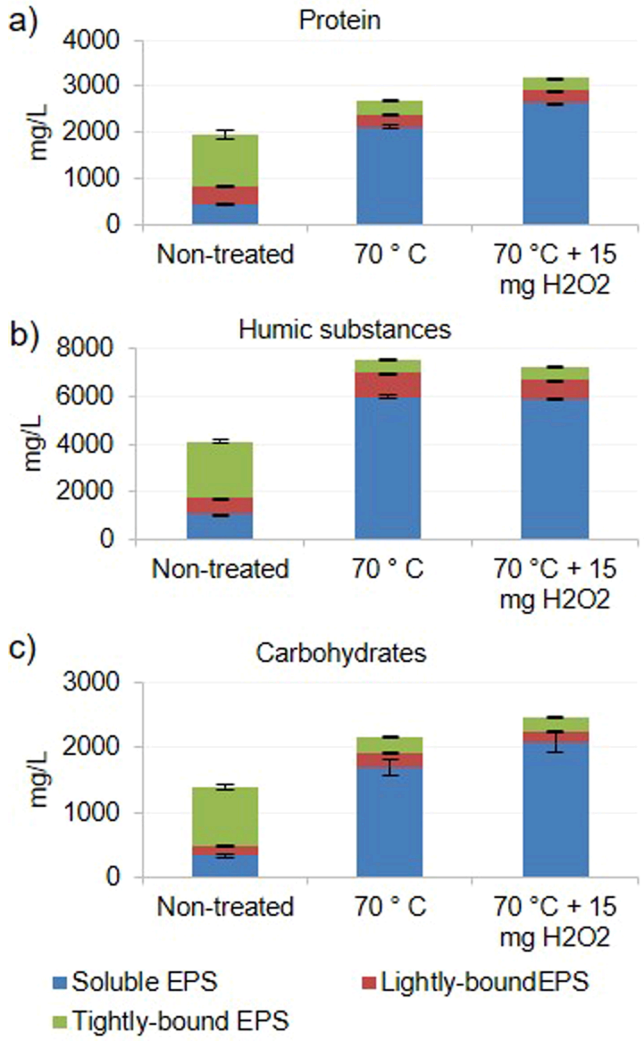

Fig. 2. Concentration and fractionation of extractable EPS into a) proteins; b) humic substances; and c) carbohydrates, applying the different treatment methods. A modification in the total measured fractions implies a change in extractable EPS upon treatment.

The effect of H_2O_2 on WAS shear stress and apparent viscosity was verified using WAS samples from two other WWTPs, i.e., Kralingseveer WWTP (KV) and Harnaschpolder WWTP (HP). From KV, 2 samples were collected with a time difference of around one month (equivalent to a 1.5 SRT in the aeration tank). The chosen pre-treatment settings were similar to our pilot study (Gonzalez et al., 2020), i.e., a temperature of 70 °C with 15 mg H_2O_2/g TS. Overall, the above-presented results seemed reproducible for both the KV and HP WAS samples (Figs. S7 and S8).

Storage (G') and loss (G'') moduli were measured to assess the effect of pre-treatment on viscoelastic properties. Fig. S9a shows that non-treated WAS required a strain of ~35% for G'' to equate G'. On the other hand, Fig. S9b and c, show that the pre-treated samples required a strain of ~17–20% to equate both moduli. This implies that a lower deformation was required to provoke a liquid-like behavior of pre-treated WAS, although very similar values were registered between WAS pre-treated at 70 °C with and without the addition of H_2O_2. This observation disagrees with the results of the other measured rheological parameters, although limitations in the analytical method (e.g., size of cone plate, heterogeneity and volume of the sample) could have played a role in this result.

The stepped dosing of H_2O_2 compared to a single-dose application

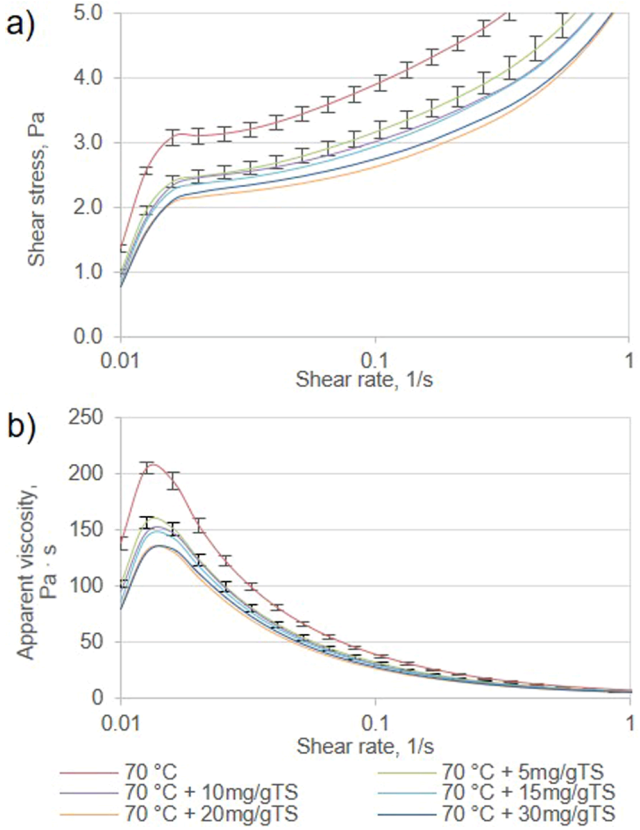

Fig. 3. a) Rheograms and; b) apparent viscosity for different pre-treatment conditions in the shear rate range 0.01–1 s^{-1}. WAS from Nieuwgraaf with TS = 61.2 g/L; n = 3.

was assessed as an approach to reduce the demand of hydrogen peroxide (Gan and Li, 2013; Pignatello et al., 2006). It was hypothesized that the partitioning of the dose into 3 events separated by 10 min could result in a higher reaction yield and would promote a more notable decrease in shear stress. However, it was observed that the stepped dosing mode had no additional effect on the decrease in shear stress (Fig. S10). Moreover, when compared to a single-dose application, the ORP of the stepped-dosed WAS did not return to reducing conditions. This implies that H_2O_2 and/or its derivatives were not completely converted during pre-treatment and the possible entrance of oxidative species into the anaerobic reactor might have occurred (Fig. S11).

3.4. Methane production rate and extent

We assessed the ability of the used pre-treatment to increase methane production of WAS, considering two possible mechanisms: a biochemical one, caused by higher accessibility of the biodegradable matter, i.e., EPS as indicated in Fig. 3 and VFA; and a physical one, induced by the modification of WAS rheology (Liu et al., 2016). The concentration of volatile fatty acids (VFAs) during AD of WAS at 35 °C is shown in Fig. S12. AD of WAS samples started with a similar VFA concentration for all conditions (Fig. S12a–c), implying that any VFAs produced during pre-treatment were diluted by the inoculum to a negligible concentration. For the pre-treated samples, the VFA concentrations increased sharply after 3 h of digestion and remained higher than the reference until hour 168 (day 7) (Fig. S12a′–c′). However, there was no clear difference in composition and only small differences in concentration of VFAs caused by the addition of H_2O_2. Overall, results suggest that VFA production was slightly stimulated by the pre-treatment. After hour 168, the VFA concentration of all samples was comparable.

Regarding methane production, Fig. 5 demonstrates that the

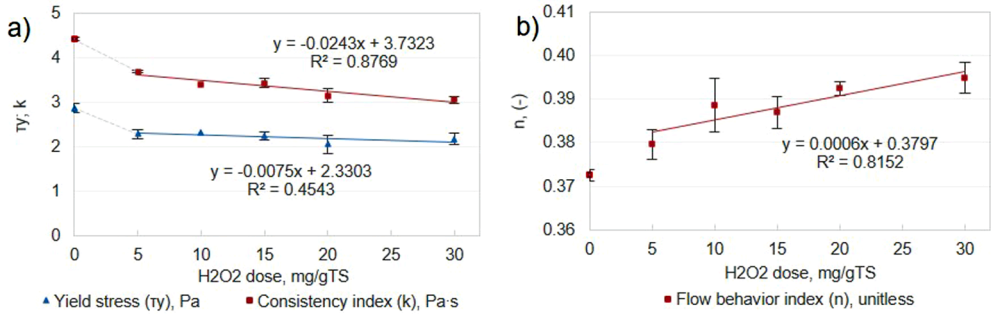

Fig. 4. Correlation between dose of H_2O_2 and a) yield stress and consistency index; and b) flow behavior index in WAS pre-treated at 70 °C; n = 3.

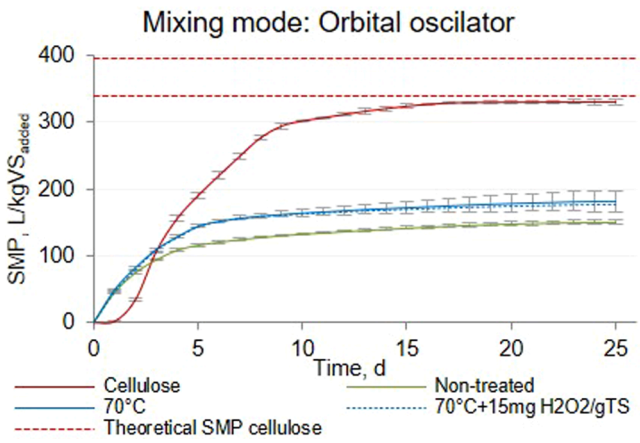

Fig. 5. SMP of cellulose and WAS at different pre-treatment conditions.

addition of H_2O_2 to WAS exposed to 70 °C did not increase its SMP compared to the sole application of temperature. However, both pre-treatment settings increased the SMP relative to the non-treated WAS, in agreement with the VFA concentrations shown in Fig. S12.

Another incubation was performed to assess the effects of mixing on methane production. The incubation was performed under two different mixing regimes: orbital shaker and stirring (using AMPTS-II motors (BPC, Sweden)). It should be noted that WAS pre-treated at 70 °C without H_2O_2 was not assayed as there was no clear difference in SMP compared to the sample including H_2O_2, as shown in Fig. 5. Additionally, the rheograms of the fermentation liquors were assessed and results are shown in Fig. S13. Fig. 6 shows the resulting SMP curves and Table 1 lists the calculated kinetic parameters.

As shown in Fig. 6 and Table 1, the samples incubated in the orbital shaker showed lower values for the kinetic parameters, suggesting non-ideal mixing conditions compared to the stirrers of the AMPTS-II (Table 1). For instance, the SMP curves of cellulose incubated in the orbital oscillator reached a plateau after ~10 days without reaching the minimum expected theoretical SMP of 340–395 $NLCH_4/kgVS_{added}$ proposed by Hafner et al., (2020). In contrast, the methane yield of the AMPTS cellulose incubations was in the expected range (Fig. 6a and b). Regarding the sludge samples, which were incubated under the orbital oscillator mixing conditions, we observed that the lower viscosity brought about by pre-treatment, resulted in increased methane production rates of the pre-treated samples compared to the non-treated ones. As a consequence, more methane was produced for the treated sample until day ~18th (Fig. 6a), although ultimately the SMP values were similar. Apparently, the pre-treatment at 70 °C with 15 mg H_2O_2/g TS improved the digester mixing conditions, resulting in enhanced mass transfer during digestion of dewatered WAS under non-ideal mixing conditions.

In addition, Fig. 6b shows an asymmetric allocation of error between different treatments in the AMPTS-II: the pre-treated samples had evidently higher standard deviations between the replicates compared with the non-treated samples. We speculate that the lower viscosity brought about by H_2O_2 made the liquor more susceptible to the variations in mixing energy from each individual AMPTS-II's motors. Moreover, any possible small difference was probably magnified since the samples were digested for 25 days. Overall, this was not the case for the orbital oscillator, which delivers the same mixing energy to all the liquors (at least conceptually).

Considering that many pilot and full-scale AD reactors are non-ideally mixed (Dapelo and Bridgeman, 2018; Wei, 2021), our present results might explain the observations done in our pilot-scale experiment, performed at similar pre-treatment settings (Gonzalez et al., 2020). In that study, pre-treatment at 70 °C with 15 mg H_2O_2/g TS, preceding compartmentalized digestion, allowed for an increase in organic loading rate from 1.4 to 4.1 kg VS/m^3d, without process impairment and even with a slight increase in biogas production (from 425 to 486 L/kg VS) and volatile solids degradation (from 40 to 44%, in absolute values). The observed increase in methane production, might be attributed to a decrease in WAS viscosity, improved mixing and enhanced mass transfer, which also coincides with the conclusion drawn by Liu et al. (2020) in a lab-scale scenario. Nonetheless, mass transfer and enhanced biochemical conversion are interrelated and were not studied as separated variables in the present study.

3.5. Possible reasons explaining the viscosity drop

3.5.1. Particle size distribution (PSD)

Changes in PSD and floc disintegration are factors that influence the apparent viscosity of biological sludge (Pevere et al., 2009; Yuan et al., 2011). While Fig. S14 shows a clear decrease in the size of particles due to the thermal effect (which seemed proportional to exposure time), no obvious additional decrease was caused by the addition of H_2O_2. Thus, the observed decrease in viscosity generated by H_2O_2 was apparently not related to changes in the average particle size of WAS.

3.5.2. Oxidative stress: Fenton's reagent

Previous studies have suggested that the effects of H_2O_2 are related to the formation of oxidative species (See Section 1). The Fenton's reagent consists of the production of hydroxyl radicals ($HO^{\bullet}$) from H_2O_2, a reaction that is catalyzed by ferrous iron (Fe^{2+}) (Eq. (5)) and its occurrence is possible at neutral pH values (Wu et al., 2020).

$$Fe^{2+} + H_2O_2 \rightarrow Fe^{3+} + HO\cdot + OH^- k \approx 70 M^{-1} s^{-1} \quad (5)$$

Thus, it was tested if the Fenton's reagent could cause the observed decrease in WAS viscosity. Based on Eq. (5) and assuming that the entire pool of iron in WAS is ferrous and accessible for H_2O_2 (27.7 ± 3.9 mg Fe/g TS, n = 3, obtained via solubilization of the WAS matrix with digestion at 300 °C with 30% HNO_3 and subsequent ICP-OES analysis), a theoretical concentration of ~7.5 mg $HO^{\bullet}$/g TS (~35 mM) was calculated. Thus, quantitatively, the possible presence of $HO^{\bullet}$ during pre-treatment

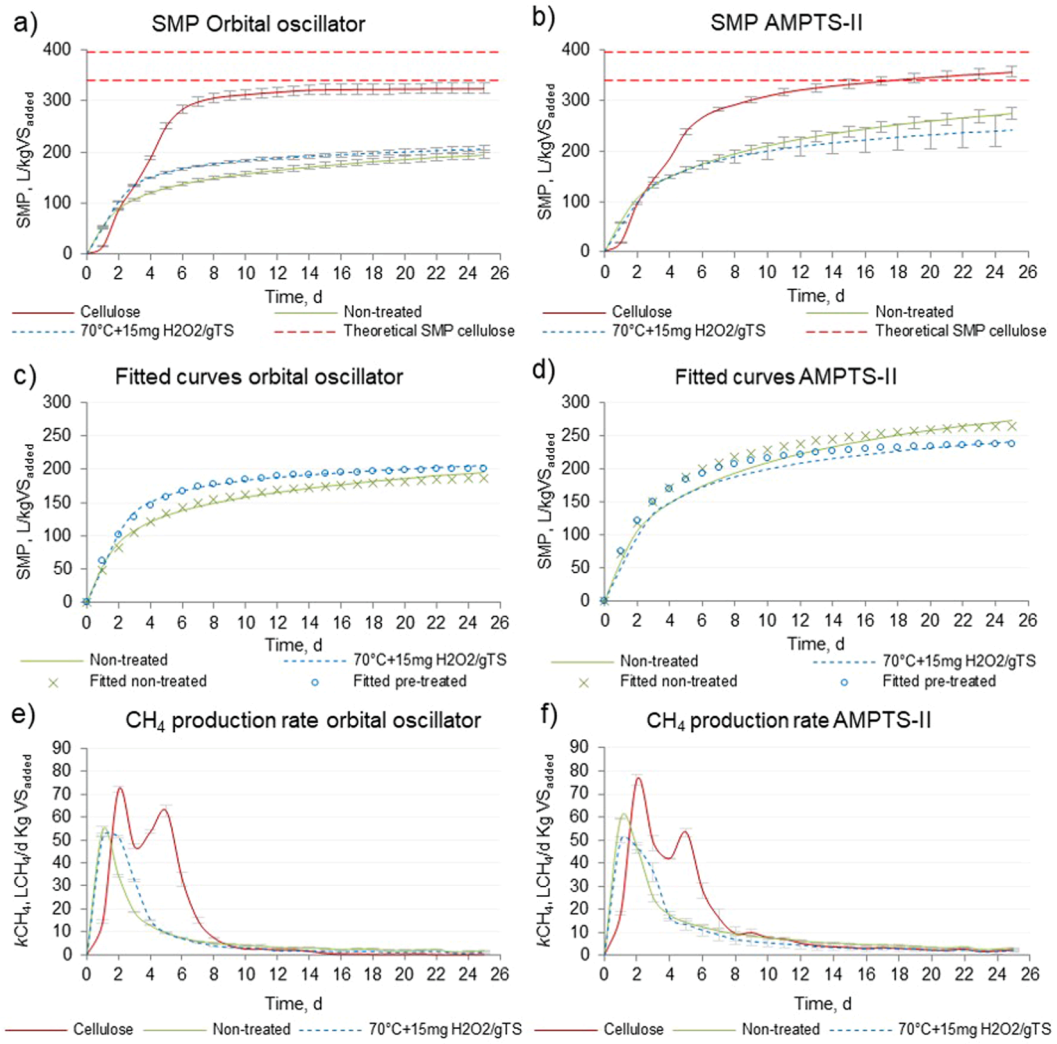

Fig. 6. SMP (a and b); fitted SMP-curves (c and d); and methane production rate (e and f), using cellulose, non-treated and pre-treated WAS as the substrate under different mixing conditions: orbital shaker (a, c and e) and AMPTS-II (b, d and f); n = 3.

Table 1
SMP kinetic parameters at different mixing conditions, n = 3.

Mixing condition	Orbital shaker			AMPTS-II		
Substrate	Cellulose	Non-treated	70 °C + 15 mg H_2O_2/g TS	Cellulose	Non-treated	70 °C + 15 mg H_2O_2/g TS
$k_{CH4\text{-}rapid}$[1], d^{-1}	–	0.44 ± 0.01	0.47 ± 0.01	–	0.51 ± 0.03	0.55 ± 0.08
$k_{CH4\text{-}slow}$[1], d^{-1}	–	0.09 ± 0.00	0.11 ± 0.01	–	0.11 ± 0.00	0.13 ± 0.02
Sum of squares, Σ(model-measured)^2		510.8	235.6		5603.7	4872.2
SMP, $NLCH_4$/kg VS_{added}	324 ± 10	195 ± 7.7	206 ± 7.2	357 ± 10.2	274 ± 12.6	242 ± 31.2
Biodegradation,%[2]	82.1 ± 2.6	36.7 ± 1.4	38.7 ± 1.3	90.3 ± 2.6	51.6. ± 2.4	45.5 ± 5.9

[1] The division between $k_{CH4\text{-}rapid}$ and $k_{CH4\text{-}slow}$ was set at the 4th day of digestion for the orbital shaker and at the 2nd day for AMPTS-II.
[2] Assuming that 1 g COD produces 0.35 L of methane.

could explain the observed changes in rheology. Fig. 7a shows the concentration of 2-hydroxyterephtalate (2hTA, which is expected to be analogous to the concentration of HO•, see Section 2.3.5) during pre-treatment of WAS. The result suggests that only 0.05% of the theoretical HO• were produced. Such a low yield could be explained by the Pourbaix diagram in Fig. S15: in the pre-treatment conditions (pH > 5.5; ORP > 0; T = ~70 °C) the dominant iron species is expected to be iron (III) oxide. Iron (III) oxides contain ferric iron (Fe^{3+}), which would result in a slower chemical pathway, as shown in Eq. (6):

$$Fe^{3+} + H_2O_2 \rightarrow Fe^{2+} + HO_2^{\cdot} + H^+ \quad k \approx 0.001 - 0.01 M^{-1}s^{-1} \tag{6}$$

Nonetheless, even a micromolar concentration of HO• suffices to provoke alterations in the physicochemical properties of proteins (Davies, 2016; Stadtman, 2001; Zhang et al., 2013), which are the most abundant organic compounds in WAS (Xu et al., 2018). A possible relationship between the production of HO• and the decrease in shear stress of sludge was assessed: Tannic acid (TA), an iron chelator (Lopes et al., 1999; Phiwchai et al., 2018), was added to WAS in a TA:Fe molar ratio of 1.5:1 to inhibit the production of HO• (Eq. (5)). As tannic acid resulted in a pH decrease of ~1 pH unit, control samples were spiked with 30% HCl to compensate for this pH drop and the resulting samples were then analyzed with fluorimetry and rheometry. Fig. 7a

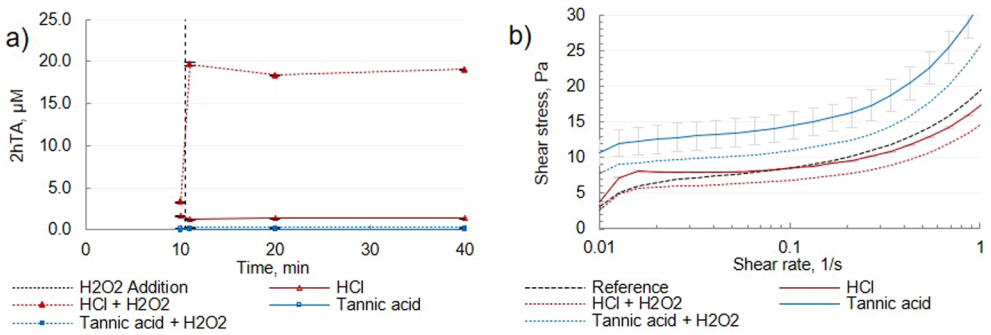

Fig. 7. a) concentration of 2hTA during pre-treatment in different conditions; b) shear rate vs shear stress curves of the pre-treated samples, n = 3.

demonstrates that tannic acid successfully inhibited the formation of 2hTA, suggesting that the Fenton's reagent was suppressed. However, despite the absence of 2hTA, the decrease in shear stress persisted when H_2O_2 was added (Fig. 7b), implying that the decrease in viscosity and the formation of HO• were unrelated (Fig. 7a). Notably, the addition of TA increased the shear stress (Fig. 7b), which was partly counteracted by adding H_2O_2.

3.5.3. *Oxidative stress: H_2O_2*

The reaction between H_2O_2 and the components of WAS (Fig. 2) might be another cause of the decrease in shear stress. Compared to HO•, H_2O_2 has a lower oxidizing potential but also higher stability (Davies, 2016; Zhang et al., 2013).

In the food science field, the combination of H_2O_2 with cationic polymers was found to increase the biocidal properties of peroxide (Rios-Castillo et al., 2017). As the WAS samples contained a cationic polymer, mixed liquor from the secondary settler was centrifuged without the use of polymer to a concentration of solids similar to the dewatered WAS with polymer. Both samples were then pre-treated and their shear stress compared. The results demonstrated that the addition of polymer was not the reason of the decrease in viscosity (Fig. S16).

However, H_2O_2 has also been demonstrated to affect specific functional groups (Wu et al., 2017): Studies from the agricultural and pharmaceutical fields proved the ability of H_2O_2 to cleave the glycosidic bonds of several polysaccharides (Dahl et al., 1998; Miller, 1986; Qin et al., 2002). Specifically, Miller (1986) demonstrated that the depolymerization caused by H_2O_2 resulted in a decrease in viscosity of a solution made of carbohydrates. An additional experiment validated this result using the pre-treatment conditions employed in the present study and solutions of collagen, humic acid sodium salt, and cellulose as model molecules for protein, humic substances, and carbohydrates (Fig. S17), which are known to be some of the most abundant organic constituents in WAS. Among them, cellulose not only had the highest viscosity (almost 3 orders of magnitude higher than the other solutions) but also was the only one that decreased its viscosity as a result of H_2O_2 addition. Thus, despite the low concentration of carbohydrates in WAS (A. Gonzalez et al., 2018), it is possible that the alteration of the molecular structure of the polysaccharides in WAS could also modify its rheology.

3.6. *Implication*

Lab-scale validation of computational fluid dynamics (CFD) models have implied an inversely proportional relation between the velocity of the particles in the digesters and the viscosity of the reactor liquor (Bridgeman, 2012; Liu et al., 2018). Liquid or sludge viscosity affects the amount of energy required to produce turbulence and to avoid dead-zones in full-scale digesters (Bridgeman, 2012; Liu et al., 2018; Wei, 2021). Since at least some rheological properties of the substrate are correlated with the properties of the digestate (Liu et al., 2016; Miryahyaei et al., 2019)(Fig. S13), a decreased yield stress of the sludge might imply less dead-zones in full scale systems.

In the present study, the use of convectional heat at 70 °C and a low dose of H_2O_2 (0.5–3% w/w), resulted in a decrease in the apparent viscosity of concentrated WAS, resulting in a more fluid sludge stream. Thus, it is considered that pre-treatment conditions are a possible strategy to increase the methane production rate of full-scale anaerobic digesters via a drop in apparent viscosity of WAS.

4. Conclusions

The results presented in this study showed that the combination of heating at 70 °C with the addition of H_2O_2 resulted in the increase in the methane production rate in non-ideally mixed anaerobic digestion. The following mechanisms were proposed to explain the phenomenon: Firstly, thermal pre-treatment at 70 °C deactivated catalase and promoted the accessibility of EPS. Thermal pre-treatment at 70 °C also increased the reaction rate of H_2O_2, which in turn lowered the apparent viscosity of WAS in the range between 5 and 30 mg H_2O_2/g TS. The decrease in viscosity of pre-treated WAS allowed a slight increase in methane production rate under non-ideal mixing conditions during anaerobic digestion.

The Fenton's reagent and the presence of conditioning agent (cationic polymer) were not related to the observed modifications in rheology. The pre-treatment conditions applied in this study might be used as a strategy to increase methane production in full-scale WAS digesters, without increasing the mixing power requirement.

CRediT authorship contribution statement

Adrian Gonzalez: Conceptualization, Formal analysis, Methodology, Investigation, Validation, Writing – original draft. **Jules B. van Lier:** Funding acquisition, Project administration, Resources, Supervision, Writing – review & editing. **Merle K. de Kreuk:** Funding acquisition, Project administration, Resources, Supervision, Writing – review & editing.

Declaration of Competing Interest

The authors declare that they have no known competing financial interests or personal relationships that could have appeared to influence the work reported in this paper.

Acknowledgements

To the Mexican National Council of Science and Technology (CONACyT) for the scholarship No. 410688 granted to the first author. We thank the four anonymous reviewers for their thorough comments and suggestions.

Funding

This work was supported by the Ministry of Economic Affairs, The

Netherlands, within the Topsector Renewable Energy funding, STOWA (project no. 432.649). The funding source had no involvement in this research.

Appendix A. Supplementary material

Supplementary data to this article can be found online at https://doi.org/10.1016/j.wasman.2022.01.017.

References

Ambrose, H.W., Chin, C.T.L., Hong, E., Philip, L., Suraishkumar, G.K., Sen, T.K., Khiadani, M., 2020. Effect of hybrid (microwave-H2O2) feed sludge pretreatment on single and two-stage anaerobic digestion efficiency of real mixed sewage sludge. Process Saf. Environ. Prot. 136, 194–202. https://doi.org/10.1016/j.psep.2020.01.032.

AntonPaar, 2021. Basics of rheology [WWW Document]. URL https://wiki.anton-paar.com/en/basics-of-rheology/ (accessed 7.7.21).

Bridgeman, J., 2012. Computational fluid dynamics modelling of sewage sludge mixing in an anaerobic digester. Adv. Eng. Softw. 44 (1), 54–62. https://doi.org/10.1016/j.advengsoft.2011.05.037.

Charbouillot, T., Brigante, M., Mailhot, G., Maddigapu, P.R., Minero, C., Vione, D., 2011. Performance and selectivity of the terephthalic acid probe for •OH as a function of temperature, pH and composition of atmospherically relevant aqueous media. J. Photochem. Photobiol. A Chem. 222 (1), 70–76. https://doi.org/10.1016/j.jphotochem.2011.05.003.

Dahl, T., He, G.-X., Samuels, G., 1998. Effect of hydrogen peroxide on the viscosity of a hydroxyethylcellulose-based gel. Pharm. Res. 15, 1137–1140. https://doi.org/10.1023/a:1011958901154.

Dapelo, D., Bridgeman, J., 2018. Euler-Lagrange computational fluid dynamics simulation of a full-scale unconfined anaerobic digester for wastewater sludge treatment. Adv. Eng. Softw. 117, 153–169. https://doi.org/10.1016/j.advengsoft.2017.08.009.

Davies, M.J., 2016. Protein oxidation and peroxidation. Biochem. J. 473, 805–825. https://doi.org/10.1042/BJ20151227.

Doskočil, L., Grasset, L., Válková, D., Pekař, M., 2014. Hydrogen peroxide oxidation of humic acids and lignite. Fuel 134, 406–413. https://doi.org/10.1016/j.fuel.2014.06.011.

Eskicioglu, C., Prorot, A., Marin, J., Droste, R.L., Kennedy, K.J., 2008. Synergetic pretreatment of sewage sludge by microwave irradiation in presence of H2O2 for enhanced anaerobic digestion. Water Res. 42 (18), 4674–4682. https://doi.org/10.1016/j.watres.2008.08.010.

Eskicioglu, C., Terzian, N., Kennedy, K., Droste, R., Hamoda, M., 2007. Athermal microwave effects for enhancing digestibility of waste activated sludge. Water Res. 41 (11), 2457–2466. https://doi.org/10.1016/j.watres.2007.03.008.

Eyster, H.C. 1950. Effect of temperature on catalase activity 273–277. [WWW Document]. URL https://kb.osu.edu/bitstream/handle/1811/3787/1/V50N06_273.pdf (accessed 1.28.22).

Fang, X., Mark, G., von Sonntag, C., 1996. OH radical formation by ultrasound in aqueous solutions Part I: the chemistry underlying the terephthalate dosimeter. Ultrason. Sonochem. 3 (1), 57–63. https://doi.org/10.1016/1350-4177(95)00032-1.

Gan, P.P., Li, S.F.Y., 2013. Efficient removal of Rhodamine B using a rice hull-based silica supported iron catalyst by Fenton-like process. Chem. Eng. J. 229, 351–363. https://doi.org/10.1016/j.cej.2013.06.020.

Gonzalez, A., Guo, H., Ortega-Ibáñez, O., Petri, C., van Lier, J.B., de Kreuk, M., Hendriks, A., 2020. Mild thermal pre-treatment of waste activated sludge to increase loading capacity, biogas production, and solids' degradation: A pilot-scale study. Energies 13, 6059. https://doi.org/10.3390/en13226059.

Gonzalez, A., Hendriks, A.T.W.M., van Lier, J.B., de Kreuk, M., 2018. Pre-treatments to enhance the biodegradability of waste activated sludge: elucidating the rate limiting step. Biotechnol. Adv. 36 (5), 1434–1469. https://doi.org/10.1016/j.biotechadv.2018.06.001.

Gonzalez, A., van Lier, J.B., de Kreuk, M.K., 2021. The role of growth media on composition, bioconversion and susceptibility for mild thermal pre-treatment of waste activated sludge. J. Environ. Manage. 298, 113491. https://doi.org/10.1016/j.jenvman.2021.113491.

Gonzalez, D., Kuang, X.M., Scott, J.A., Rocha, G.O., Paulson, S.E., Gonzalez, D.H., Kuang, X.M., Scott, J.A., Olimpio, G., 2018. Terephthalate probe for hydroxyl radicals: yield of 2-hydroxyterephthalic acid and transition metal interference. Anal. Lett. 51, 2488–2497. https://doi.org/10.1080/00032719.2018.1431246.

Hafner, S.D., Fruteau de Laclos, H., Koch, K., Holliger, C., 2020. Improving inter-laboratory reproducibility in measurement of biochemical methane potential (BMP). Water 12 (6), 1752. https://doi.org/10.3390/w12061752.

Hammadi, L., Ponton, A., Belhadri, M., 2012. Effects of heat treatment and hydrogen peroxide (H2O2) on the physicochemical and rheological behavior of an activated sludge from a water purification plant. Procedia Eng. 33, 293–302. https://doi.org/10.1016/j.proeng.2012.01.1207.

Iwase, T., Tajima, A., Sugimoto, S., Okuda, K.-I., Hironaka, I., Kamata, Y., Takada, K., Mizunoe, Y., 2013. A simple assay for measuring catalase activity: a visual approach. Sci. Rep. 3 (1) https://doi.org/10.1038/srep03081.

Le, N.T., Julcour-Lebigue, C., Delmas, H., 2015. An executive review of sludge pretreatment by sonication. J. Environ. Sci. (China) 37, 139–153. https://doi.org/10.1016/j.jes.2015.05.031.

Liang, J., Zhang, S., Huang, J., Ye, M., Yang, X., Huang, S., Sun, S., 2020. Mechanism of zero valent iron and anaerobic mesophilic digestion combined with hydrogen peroxide pretreatment to enhance sludge dewaterability: relationship between soluble EPS and rheological behavior. Chemosphere 247, 125859. https://doi.org/10.1016/j.chemosphere.2020.125859.

Liu, J., Jia, R., Wang, Y., Wei, Y., Zhang, J., Wang, R., Cai, X., 2015. Does residual H2O2 result in inhibitory effect on enhanced anaerobic digestion of sludge pretreated by microwave-H2O2 pretreatment process? Environ. Sci. Pollut. Res. 24 (10), 9016–9025. https://doi.org/10.1007/s11356-015-5704-z.

Liu, J., Yang, M., Zhang, J., Zheng, J., Xu, H., Wang, Y., Wei, Y., 2018. A comprehensive insight into the effects of microwave-H2O2 pretreatment on concentrated sewage sludge anaerobic digestion based on semi-continuous operation. Bioresour. Technol. 256, 118–127. https://doi.org/10.1016/j.biortech.2018.01.126.

Liu, J., Yu, D., Zhang, J., Yang, M., Wang, Y., Wei, Y., Tong, J., 2016. Rheological properties of sewage sludge during enhanced anaerobic digestion with microwave-H2O2 pretreatment. Water Res. 98, 98–108. https://doi.org/10.1016/j.watres.2016.03.073.

Liu, J., Zheng, J., Zhang, J., Yu, D., Wei, Y., 2020. The performance evaluation and kinetics response of advanced anaerobic digestion for sewage sludge under different SRT during semi-continuous operation. Bioresour. Technol. 308, 123239. https://doi.org/10.1016/j.biortech.2020.123239.

Lopes, G.K.B., Schulman, H.M., Hermes-Lima, M., 1999. Polyphenol tannic acid inhibits hydroxyl radical formation from Fenton reaction by complexing ferrous ions. Biochim. Biophys. Acta 1472, 142–152. https://doi.org/10.1016/S0304-4165(99)00117-8.

Miller, A.R., 1986. Oxidation of cell wall polysaccharides by hydrogen peroxide: A potential mechanism for cell wall breakdown in plants. Biochem. Biophys. Res. Commun. 141 (1), 238–244. https://doi.org/10.1016/S0006-291X(86)80359-X.

Miryahyaei, S., Olinga, K., Abdul Muthalib, F.A., Das, T., Ab Aziz, M.S., Othman, M., Baudez, J.C., Batstone, D., Eshtiaghi, N., 2019. Impact of rheological properties of substrate on anaerobic digestion and digestate dewaterability: New insights through rheological and physico-chemical interaction. Water Res. 150, 56–67. https://doi.org/10.1016/j.watres.2018.11.049.

Neumann, P., Pesante, S., Venegas, M., Vidal, G., 2016. Developments in pre-treatment methods to improve anaerobic digestion of sewage sludge. Rev. Environ. Sci. Biotechnol. 15 (2), 173–211. https://doi.org/10.1007/s11157-016-9396-8.

Pevere, A., Guibaud, G., Goin, E., van Hullebusch, E., Lens, P., 2009. Effects of physico-chemical factors on the viscosity evolution of anaerobic granular sludge. Biochem. Eng. J. 43 (3), 231–238. https://doi.org/10.1016/j.bej.2008.10.003.

Phiwchai, I., Yuensook, W., Sawaengsiriphon, N., Krungchanuchat, S., Pilapong, C., 2018. Tannic acid (TA): A molecular tool for chelating and imaging labile iron. Eur. J. Pharm. Sci. 114, 64–73. https://doi.org/10.1016/j.ejps.2017.12.004.

Pignatello, J.J., Oliveros, E., MacKay, A., 2006. Advanced oxidation processes for organic contaminant destruction based on the Fenton reaction and related chemistry. Crit. Rev. Environ. Sci. Technol. 36 (1), 1–84. https://doi.org/10.1080/10643380500326564.

Pilli, S., Bhunia, P., Yan, S., LeBlanc, R.J., Tyagi, R.D., Surampalli, R.Y., 2011. Ultrasonic pretreatment of sludge: a review. Ultrason. Sonochem. 18 (1), 1–18. https://doi.org/10.1016/j.ultsonch.2010.02.014.

Pilli, S., Yan, S., Tyagi, R.D., Surampalli, R.Y., 2014. Thermal pretreatment of sewage sludge to enhance anaerobic digestion: A review. Crit. Rev. Environ. Sci. Technol. 45 (6), 669–702. https://doi.org/10.1080/10643389.2013.876527.

Qin, C.Q., Du, Y.M., Xiao, L., 2002. Effect of hydrogen peroxide treatment on the molecular weight and structure of chitosan. Polym. Degrad. Stab. 76 (2), 211–218. https://doi.org/10.1016/S0141-3910(02)00016-2.

Ratkovich, N., Horn, W., Helmus, F.P., Rosenberger, S., Naessens, W., Nopens, I., Bentzen, T.R., 2012. Activated sludge rheology: A critical review on data collection and modelling. Water Res. 47 (2), 463–482. https://doi.org/10.1016/j.watres.2012.11.021.

Ríos-Castillo, A.G., González-Rivas, F., Rodríguez-Jerez, J.J., 2017. Bactericidal efficacy of hydrogen peroxide-based disinfectants against gram-positive and gram-negative bacteria on stainless steel surfaces. Food Microbiol. Saf. 82 (10), 2351–2356. https://doi.org/10.1111/1750-3841.13790.

Samstag, R.W., Ducoste, J.J., Griborio, A., Nopens, I., Batstone, D.J., Wicks, J.D., Saunders, S., Wicklein, E.A., Kenny, G., Laurent, J., 2016. CFD for wastewater treatment: An overview. Water Sci. Technol. 74, 549–563. https://doi.org/10.2166/wst.2016.249.

Stadtman, E.R., 2001. Protein oxidation in aging and age-related diseases. Ann. N. Y. Acad. Sci. 928, 22–38. https://doi.org/10.1111/j.1749-6632.2001.tb05632.x.

Velayati, A.A., Farnia, P., Saif, S., 2019. Identification of nontuberculous Mycobacterium: Conventional versus rapid molecular tests. In: Nontuberculous Mycobacteria (NTM). Elsevier Inc, pp. 11–59. https://doi.org/10.1016/B978-0-12-814692-7.00002-4.

Wang, Y., Wei, Y., Liu, J., 2009. Effect of H2O2 dosing strategy on sludge pretreatment by microwave-H2O2 advanced oxidation process. J. Hazard. Mater. 169 (1-3), 680–684. https://doi.org/10.1016/j.jhazmat.2009.04.001.

Wei, P. 2021. Characterisation of Sludge Rheology and Sludge Mixing in Gas-mixed Anaerobic Digesters. Doctoral Thesis. Delft University of Technology. doi:10.4233/uuid:ab767694-02ee-49a4-a35d-f3eb7daaf538.

Wei, P., Mudde, R.F., Uijttewaal, W., Spanjers, H., van Lier, J.B., de Kreuk, M., 2019. Characterising the two-phase flow and mixing performance in a gas-mixed anaerobic digester: Importance for scaled-up applications. Water Res. 149, 86–97. https://doi.org/10.1016/j.watres.2018.10.077.

Wei, P., Tan, Q., Uijttewaal, W., Lier, J.B.V., Kreuk, M.D., 2018. Experimental and mathematical characterisation of the rheological instability of concentrated waste

activated sludge subject to anaerobic digestion. Chem. Eng. J. 349, 318–326. https://doi.org/10.1016/j.cej.2018.04.108.

Wei, P., Uijttewaal, W., van Lier, J.B., de Kreuk, M., 2021. Impacts of shearing and temperature on sewage sludge: Rheological characterisation and integration to flow assessment. Sci. Total Environ. 774, 145005. https://doi.org/10.1016/j.scitotenv.2021.145005.

Wu, B., Dai, X., Chai, X., 2020. Critical review on dewatering of sewage sludge: Influential mechanism, conditioning technologies and implications to sludge re-utilizations. Water Res. 180, 115912. https://doi.org/10.1016/j.watres.2020.115912.

Wu, B., Ni, B.-J., Horvat, K., Song, L., Chai, X., Dai, X., Mahajan, D., 2017. Occurrence state and molecular structure analysis of extracellular proteins with implications on the dewaterability of waste-activated sludge. Environ. Sci. Technol. 51 (16), 9235–9243. https://doi.org/10.1021/acs.est.7b0286110.1021/acs.est.7b02861.s001.

Wu, D., Qian, X., 2018. Experimental study on the thermal runaway of hydrogen peroxide with in-/organic impurities by a batch reactor. J. Loss Prev. Process Ind. 51, 200–207. https://doi.org/10.1016/j.jlp.2017.12.012.

Xiao, Q., Yan, H., Wei, Y., Wang, Y., Zeng, F., Zheng, X., 2012. Optimization of H2O2 dosage in microwave-H2O2 process for sludge pretreatment with uniform design method. J. Environ. Sci. (China) 24 (12), 2060–2067. https://doi.org/10.1016/S1001-0742(11)60998-4.

Xu, Q., Wang, Q., Zhang, W., Yang, P., Du, Y., Wang, D., 2018. Highly effective enhancement of waste activated sludge dewaterability by altering proteins properties using methanol solution coupled with inorganic coagulants. Water Res. 138, 181–191. https://doi.org/10.1016/j.watres.2018.03.038.

Yu, W., Yang, J., Shi, Y., Song, J., Shi, Y., Xiao, J., Li, C., Xu, X., He, S., Liang, S., Wu, X., Hu, J., 2016. Roles of iron species and pH optimization on sewage sludge conditioning with Fenton's reagent and lime. Water Res. 95, 124–133. https://doi.org/10.1016/j.watres.2016.03.016.

Yuan, H.-P., Yan, X.-F., Yang, C.-F., Zhu, N.-W., 2011. Enhancement of waste activated sludge dewaterability by electro-chemical pretreatment. J. Hazard. Mater. 187 (1-3), 82–88. https://doi.org/10.1016/j.jhazmat.2010.12.106.

Zhang, W., Xiao, S., Ahn, D.U., 2013. Protein oxidation: basic principles and implications for meat quality. Crit. Rev. Food Sci. Nutr. 53 (11), 1191–1201. https://doi.org/10.1080/10408398.2011.577540.

Zhen, G., Wang, J., Lu, X., Su, L., Zhu, X., Zhou, T., Zhao, Y., 2019. Effective gel-like floc matrix destruction and water seepage for enhancing waste activated sludge dewaterability under hybrid microwave-initiated Fe(II)-persulfate oxidation process. Chemosphere 221, 141–153. https://doi.org/10.1016/j.chemosphere.2019.01.037.